Physiological and Molecular Determinants of Insulin Action in the Baboon

Alberto O. Chavez,[1] Juan C. Lopez-Alvarenga,[2,3] M. Elizabeth Tejero,[2] Curtis Triplitt,[1] Raul A. Bastarrachea,[2,3] Apiradee Sriwijitkamol,[1] Puntip Tantiwong,[1] V. Saroja Voruganti,[2] Nicolas Musi,[1] Anthony G. Comuzzie,[2,3] Ralph A. DeFronzo,[1] and Franco Folli[1,2]

OBJECTIVE—To quantitate insulin sensitivity in lean and obese nondiabetic baboons and examine the underlying cellular/molecular mechanisms responsible for impaired insulin action to characterize a baboon model of insulin resistance.

RESEARCH DESIGN AND METHODS—Twenty baboons received a hyperinsulinemic-euglycemic clamp with skeletal muscle and visceral adipose tissue biopsies at baseline and at 30 and 120 min after insulin. Genes and protein expression of key molecules involved in the insulin signaling cascade (insulin receptor, insulin receptor substrate-1, p85, phosphatidylinositol 3-kinase, Akt, and AS160) were sequenced, and insulin-mediated changes were analyzed.

RESULTS—Overall, baboons show a wide range of insulin sensitivity (6.2 ± 4.8 mg $\cdot$ kg^{-1} $\cdot$ min^{-1}), and there is a strong inverse correlation between indexes of adiposity and insulin sensitivity ($r = -0.946$, $P < 0.001$ for % body fat; $r = -0.72$, $P < 0.001$ for waist circumference). The genes and protein sequences analyzed were found to have ~98% identity to those of man. Insulin-mediated changes in key signaling molecules were impaired both in muscle and adipose tissue in obese insulin-resistant compared with lean insulin-sensitive baboons.

CONCLUSIONS—The obese baboon is a pertinent nonhuman primate model to examine the underlying cellular/molecular mechanisms responsible for insulin resistance and eventual development of type 2 diabetes. ***Diabetes*** **57:899–908, 2008**

Insulin resistance is characterized by impaired response of target organs (e.g., skeletal muscle, liver, adipose tissue, and heart) to the physiological effects of insulin and results in impaired glucose metabolism. Insulin resistance is a characteristic feature of many common metabolic disorders, including obesity, type 2 diabetes, hypertension, and dyslipidemia, and of the normal aging process, which collectively constitute risk factors for the development of atherosclerotic cardiovascular disease (1–3).

Nonhuman primates occupy a unique place in biomedical and evolutionary research by virtue of their close genetic and physiological similarity to humans and represent a valuable model that has great relevance to the study of human disease. Old World monkeys, which recently (~25 millions years ago in evolutionary terms) diverged from the Hominoidea, have been most extensively studied (4,5). This taxonomic group includes vervet monkeys (*Chlorocebus aethiops*), rhesus macaques (*Macaca mulatta*), cynomolgus monkeys (*Macaca fascicularis*), and baboons (*Papio hamadryas*) (6). Despite the relevance of primate study to human disease research, there has been a shortage of primates available for biomedical research (7). Baboons and humans share great genetic similarity, with ~96% homology evident at the DNA level (8). The sequences of specific genes and the arrangements of genetic loci on chromosomes reflect the close evolutionary relationship between these two species (9). Not surprisingly, nonhuman primates develop many diseases similar to those in man, and they have been used as a model for osteoporosis, lipoprotein, and atherosclerosis research (10–12) and most recently, to study the genetics of obesity (4,13).

Baboons are long-lived animals with an average lifespan of ~25 years. They can be maintained for generations in controlled conditions, thus providing a valuable model for studying interactions between inherited, constitutional, and environmental factors such as diet and exercise (12,14,15). There are no established glycemic cut points for the diagnosis of diabetes in the baboon. Nonetheless, the development of overt type 2 diabetes is well documented (16–18), although the exact incidence remains to be determined. The natural history of type 2 diabetes in baboons is likely to parallel the natural history that has been observed in other primates (6,19,20) and in humans (1). Thus, as baboons gain excessive weight, they become insulin resistant and glucose intolerant. Therefore, we sought to quantitate insulin sensitivity in a population of nondiabetic baboons using the hyperinsulinemic-euglycemic clamp to characterize the clinical and biochemical characteristics of insulin-resistant baboons and to examine the underlying cellular/molecular mechanisms responsible for the impairment in insulin action.

RESEARCH DESIGN AND METHODS

Study population. Twenty nondiabetic baboons (10 males and 10 females) randomly selected from the Southwest National Primate Research Center at Southwest Foundation for Biomedical Research (San Antonio, TX) were studied. As part of the initial evaluation, baseline anthropometric measurements and biochemical profiles, including fasting plasma glucose (FPG) and A1C, were measured. Only baboons with stable weight pattern (<3% weight

From the [1]Diabetes Division, University of Texas Health Science Center at San Antonio, San Antonio, Texas; the [2]Genetics Department, Southwest Foundation for Biomedical Research, San Antonio, Texas; and the [3]Southwest National Primate Research Center, San Antonio, Texas.

Address correspondence and reprint requests to Franco Folli, MD, PhD, Diabetes Division, Department of Medicine, The University of Texas Health Science Center at San Antonio, 7703 Floyd Curl Dr., San Antonio, TX 78229. E-mail: folli@uthscsa.edu.

Received for publication 8 June 2007 and accepted in revised form 23 December 2007.

Published ahead of print at http://diabetes.diabetesjournals.org on 3 January 2008. DOI: 10.2337/db07-0790.

FFA, free fatty acid; FFM, fat-free mass; FPG, fasting plasma glucose; FPI, fasting plasma insulin; HOMA-β, homeostasis model assessment of β-cell function; HOMA-IR, homeostasis model assessment of insulin resistance; IRS, insulin receptor substrate; PI 3-kinase, phosphatidylinositol 3-kinase; R_d, glucose disposal rate.

TABLE 1
Clinical, anthropometric, laboratory, and glucose metabolic characteristics of the baboons

	Total population	Females	Males	*P* value
n	20	10	10	
Age (years)	19.3 ± 6.0	20.6 ± 5.9	18.2 ± 6.4	0.399
Weight (kg)	25.2 ± 5.6	22.8 ± 6.4	27.7 ± 3.5	0.054
Height (crown to heel) (cm)	100.7 ± 7.9	94.0 ± 5.3	106.8 ± 4.1	0.001
Waist (cm)	56.1 ± 10.5	59.1 ± 14	53.6 ± 5.5	0.295
BMI (kg/m^2)	24.4 ± 4.8	24.6 ± 6.5	24.3 ± 3.1	0.891
% Body fat	10.9 ± 9.4	11.7 ± 2.3	6.2 ± 1.5	0.05
FPG (mg/dl)	105 ± 21	110 ± 22	100 ± 20	0.263
A1C (%)	4.7 ± 0.6	4.8 ± 0.7	4.6 ± 0.5	0.354
Cholesterol				
Total (mg/dl)	89 ± 28	99 ± 30	78 ± 22	0.094
HDL (mg/dl)	46 ± 11	45 ± 10	46 ± 13	0.837
LDL (mg/dl)	34 ± 19	42 ± 22	26 ± 10	0.053
TG (mg/dl)	47 ± 24	62 ± 25.6	32 ± 10	0.002
FPI (μU/ml)	16 ± 13	23 ± 14	8 ± 6	0.007
F-C Peptide (ng/ml)	2 ± 1	2.3 ± 1.1	1.6 ± 0.8	0.15
F-FFA (μEq/l)	532 ± 27	697 ± 23	385 ± 23	0.009
SSPI (μU/ml)	231 ± 60	246 ± 65	215 ± 60	0.28
ΔPI (μU/ml)	215 ± 57	223 ± 56	207 ± 60	0.54
SSPG (mg/dl)	89 ± 3	89 ± 4	89 ± 2	0.94
$FFA_{90–120}$ (μEq/l)	233 ± 16	358 ± 16	121 ± 16	0.002
$R_{d90–120}$ (mg · kg^{-1} · min^{-1})	6.2 ± 4.8	6.7 ± 6.4	5.7 ± 3.0	0.663
HOMA-IR	4.4 ± 4	6.9 ± 4.6	2.1 ± 1.6	0.009
HOMA-β (%)	137 ± 86	180 ± 77	94 ± 75	0.015

Data are expressed as means ± SD. TG, triglycerides; SSPI, steady-state plasma insulin concentration during insulin clamp; ΔPI, increment in plasma insulin concentration during insulin clamp; SSPG, steady-state plasma glucose concentration during insulin clamp; F, fasting.

change over the preceding 12 months), according to biannual health check records, were studied. All animals had normal screening laboratory tests and an A1C <6%. The animals were fed an ad libitum chow diet containing 75.4% carbohydrates, 17.7% protein, and 6.9% fat (Teklad 15% Monkey Diet; Harlan, Indianapolis, IN) and housed in corrals, where they performed unrestrained physical activity.

Body composition analysis. All baboons underwent a dual-energy X-ray absorptiometry scan (Lunar Prodigy Whole Body Scanner; GE Medical Systems, Madison, WI) to determine fat-free mass (FFM), fat mass, and percent body fat. Scanning time was ~5 min and was performed under sedation.

Hyperinsulinemic-euglycemic clamp, skeletal muscle, and visceral fat biopsies. Insulin sensitivity was assessed with the euglycemic insulin clamp technique as previously described (21). After an overnight fast (~12 h), each baboon was sedated with ketamine hydrochloride (10 mg/kg i.m.) before arrival in the procedure room. Endotracheal intubation was performed using disposable cuffed tubes (6.5–8.0 mm diameter) under direct laryngoscopic visualization, and all the animals were supported with 98–99.5% FiO_2 by a pressure controlled ventilator adjusted, as necessary, to keep the oxygen saturation >95%. The maintenance of anesthesia consisted of an inhaled isofluorane (0.5–1.5%) and oxygen mix. Catheters were inserted into the femoral vein for insulin and glucose infusion and into the contralateral femoral artery for blood sampling. FPG, free fatty acid (FFA), and insulin concentrations were measured at −10 and 0 min. At $t = 0$ min, a primed-continuous infusion of human regular insulin (Novolin; Novo Nordisk, Princeton, NJ) was started and continued at 60 mU/m^2 body surface area per minute for 120 min. Body surface area (A) was estimated from the body mass (M) by the Meeh formula $A = K.M^{2/3}$, in which the constant $K = 12.65$, as proposed by van As and Lombard (22) for the baboon. After the start of insulin, plasma glucose was measured every 5 min, and the infusion of 20% glucose solution was adjusted, based on the negative feedback principle, to maintain the plasma glucose concentration at the desired level of ~90 mg/dl. Plasma insulin and FFA concentrations were measured at 30, 60, 90, 100, 110, and 120 min. At −60 min and at 30 and 120 min during the insulin clamp, open *Vastus lateralis* skeletal muscle biopsies and abdominal subcutaneous and visceral fat biopsies were obtained. Five hundred milligrams skeletal muscle and ~1 g adipose tissue were obtained per biopsy. Tissues were blotted free from blood, immediately frozen, and stored at −80°C until use.

Analytical determinations. Plasma glucose was measured by glucose oxidase method using Beckman Glucose Analyzer 2 (Beckman-Coulter, Fullerton, CA). A1C and plasma lipids were measured with commercial kits in an ACE Clinical Chemistry System (Alfa Wassermann Diagnostic Technologies, NJ). Plasma insulin was measured by radioimmunoassay (Diagnostic Products, Los Angeles, CA) and plasma FFA with an enzymatic colorimetric assay (Wako Chemicals USA)

Immunoprecipitation and immunoblotting. Immunoprecipitation and Western blotting were performed as previously described (23,24) and are detailed in the online appendix.

Electron microscopy. Immediately after biopsies, skeletal muscle from each baboon was cut in small sections (~1 × 1 × 2 mm), fixed in phosphate-buffered 4% formaldehyde-1% glutaraldehyde overnight, postfixed in 1% osmium tetroxide, dehydrated, and embedded in Epon resin. Sections ~500 nm of thickness were cut and mounted in copper grids and finally stained with uranyl acetate and lead citrate as previously described (25). Sections were scoped in JEOL JEM-1230 microscope, and images at magnification ×15,000 and ×40,000 were acquired and stored digitally. Ten random pictures (×15,000, each one covering an area of 90 μm^2 of muscle) were analyzed to measure total area occupied by mitochondria, number of mitochondria per area, and average area per mitochondria using an image analysis software (ImageJ 1.37v; National Institutes of Health).

Cloning and sequencing of baboon insulin signaling molecules. Cloning and sequencing methods of baboon insulin-signaling proteins are detailed in the online appendix.

Calculations. During the euglycemic insulin clamp, insulin sensitivity was calculated as the mean rate of insulin-stimulated whole-body glucose disposal (R_d) during the 90–120 time periods, because at the prevailing level of hyperinsulinemia, endogenous glucose production is completely suppressed (26,27). Insulin resistance measured by homeostasis model assessment (HOMA-IR) was calculated as fasting plasma insulin (FPI; microunits/milliliter) × FPG (millimoles/liter)/22.5. HOMA of β-cell function (HOMA-β) was estimated as FPI (microunits/milliliter) × 20/FPG (millimoles/liter) − 3.5, as reported by Matthews et al. (28).

Statistical analysis. Statistical calculations were performed with SPSS for Windows (version 9.0; SPSS, Chicago, IL). All data are expressed as means ± SD. Measured parameters found to have positive skewness were transformed to natural logarithms. Student's t test was used for comparisons between sexes. Multiple linear regressions were used to adjust explanatory variables for sex and age. We made a conservative approach adjusting the coefficient of determination (r^2) by the number of explanatory variables. This approach provides the explained percent of variance after the contribution of chance is

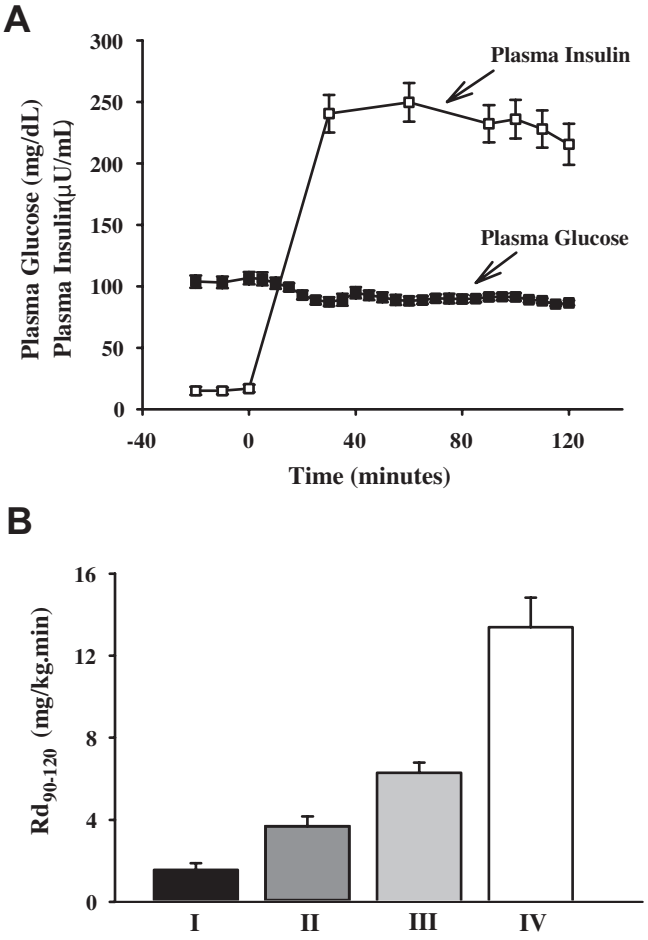

FIG. 1. *A*: Time course of plasma insulin and glucose concentrations during the euglycemic insulin clamp studies (n = 20). Data represent the means ± SE. *B*: Quartiles (n = 5 per group) of insulin sensitivity based on the insulin-stimulated R_d ($R_{d90–120}$) during the euglycemic insulin clamp. Group I represents the most insulin-resistant animals (black bar). Group IV (n = 5) represents the most insulin-sensitive baboons (white bar).

subtracted. The β-coefficients were standardized to judge relative predictive power of independent variables, and partial correlations were calculated to remove the overlap effect between variables. Finally, mean adjusted predictions were calculated for R_d using the significant regression equations.

RESULTS

Characteristics of the study population are summarized in Table 1. Body weight (27.7 ± 3.5 vs. 22.8 ± 6.4 kg, P = 0.05) and height (106.8 ± 4.1 vs. 94.0 ± 5.3 cm, $P < 0.001$) were significantly different in males and females. However, the BMI was similar in males (24.3 ± 3.1 kg/m^2) and females (24.6 ± 6.5 kg/m^2) (P = 0.89). Waist circumference also was similar in males and females (53.6 ± 5.5 vs. 59.1 ± 14 cm, respectively, P = 0.30). FPG, A1C, and insulin-stimulated R_d were similar in males and females. Fasting plasma insulin concentration and HOMA-IR were significantly greater in females than males. No sex differences in total cholesterol and HDL cholesterol were observed. However, plasma LDL cholesterol, triglycerides, and FFAs were significantly greater in females than males (Table 1).

Hyperinsulinemic-euglycemic clamp studies. Steady-state plasma glucose concentration during the insulin clamp was 89 ± 3 with a coefficient of variation <5% in all studies (Table 1; Fig. 1). Both the steady-state plasma insulin concentration and increment in plasma insulin concentration above baseline during the clamp were similar in males and females (Table 1). The insulin-stimulated R_d during euglycemic insulin clamp was not significantly different between males (5.7 ± 3.0 mg · kg^{-1} · min^{-1}) and females (6.7 ± 6.4 mg · kg^{-1} · min^{-1}) (P = 0.633). However, a wide range of insulin sensitivity was found in the study population. According to the cut off values for insulin-sensitive (R_d >6.0 mg · kg^{-1} · min^{-1}) and insulin-resistant (R_d <4.0 mg · kg^{-1} · min^{-1}) baboons, eight baboons were included in the insulin-resistant category and eight in the insulin-sensitive category. When divided into equal quartiles containing five baboons per quartile, a sevenfold difference in insulin-stimulated R_d was observed (Fig. 1).

Relation between measures of adiposity. Waist circumference, adjusted for age and sex, was strongly and positively correlated with percent body fat in the population (r = 0.912, $P < 0.01$) (Fig. 2*D*). Waist circumference also was highly correlated with BMI (r = 0.865, P = 0.002). Percent body fat and BMI also were significantly correlated (r = 0.629, P = 0.007).

Relationship between insulin sensitivity, metabolic parameters, and adiposity indexes. Using stepwise linear regression analysis (threshold of $P > 0.10$ to be removed from the analysis), including age, sex, BMI, waist circumference, percent body fat (log transformed), FFM, HOMA-IR, FPI, A1C, FPG, HDL cholesterol, triglycerides, and LDL cholesterol, the best predictors of insulin sensitivity (adjusted for sex) were percent body fat (r = −0.946, $P < 0.001$), waist circumference (r = −0.72, $P <$ 0.001), and A1C (r = −0.67, $P < 0.01$) (Fig. 2). The overall r^2 of the model was 0.893.

According to this predictive model, insulin-stimulated R_d decreased by 0.38 mg · kg^{-1} · min^{-1} per centimeter increase in waist circumference and by 0.67 mg · kg^{-1} · min^{-1} for each percent increase in body fat. There was a strong correlation between the predicted and observed values in the model, both for the percent body fat and waist circumference (data not shown).

We performed a multivariate analysis to explain R_d values related to FFA and anthropometric measurements. The initial FFA effect, adjusted by sex and age over R_d was $r_{partial}$ = −0.566, P = 0.02. When we added waist circumference and percent body fat, all adjusted by age and sex, FFA ($r_{partial}$ = 0.37, P = 0.19) lost its effect in the presence of percent body fat ($r_{partial}$ = −0.78, P = 0.001) and waist circumference ($r_{partial}$ = −0.95, P = 0.01). The total adjusted r^2 of this model was 0.82.

Estimates of β-cell function. In the fasting state, C-peptide levels were not significantly different by sex (P = 0.15; Table 1). However, significant sex differences were found in estimated β-cell function when calculated with the HOMA-β index (180 ± 77% males vs. 94 ± 75% females, $P < 0.05$). HOMA-β also was inversely correlated with HOMA-IR (r = 0.651, $P < 0.01$), fasting FFA (r = 0.616, $P < 0.01$), and percent body fat (r = 0.519, $P < 0.05$) (Table 2).

Insulin signaling measurements. Baboons were divided into insulin-sensitive and insulin-resistant groups based on an R_d >6.0 or <4.0 mg · kg^{-1} · min^{-1}. In the skeletal muscle of insulin-sensitive baboons, insulin receptor substrate-1 (IRS-1) tyrosine phosphorylation increased significantly at 30 min compared with basal ($P < 0.05$), whereas there was no significant stimulation in the insulin-resistant group (Fig. 3*A*). IRS-1–associated p85 increased maximally at 30 min in the insulin-sensitive group compared with

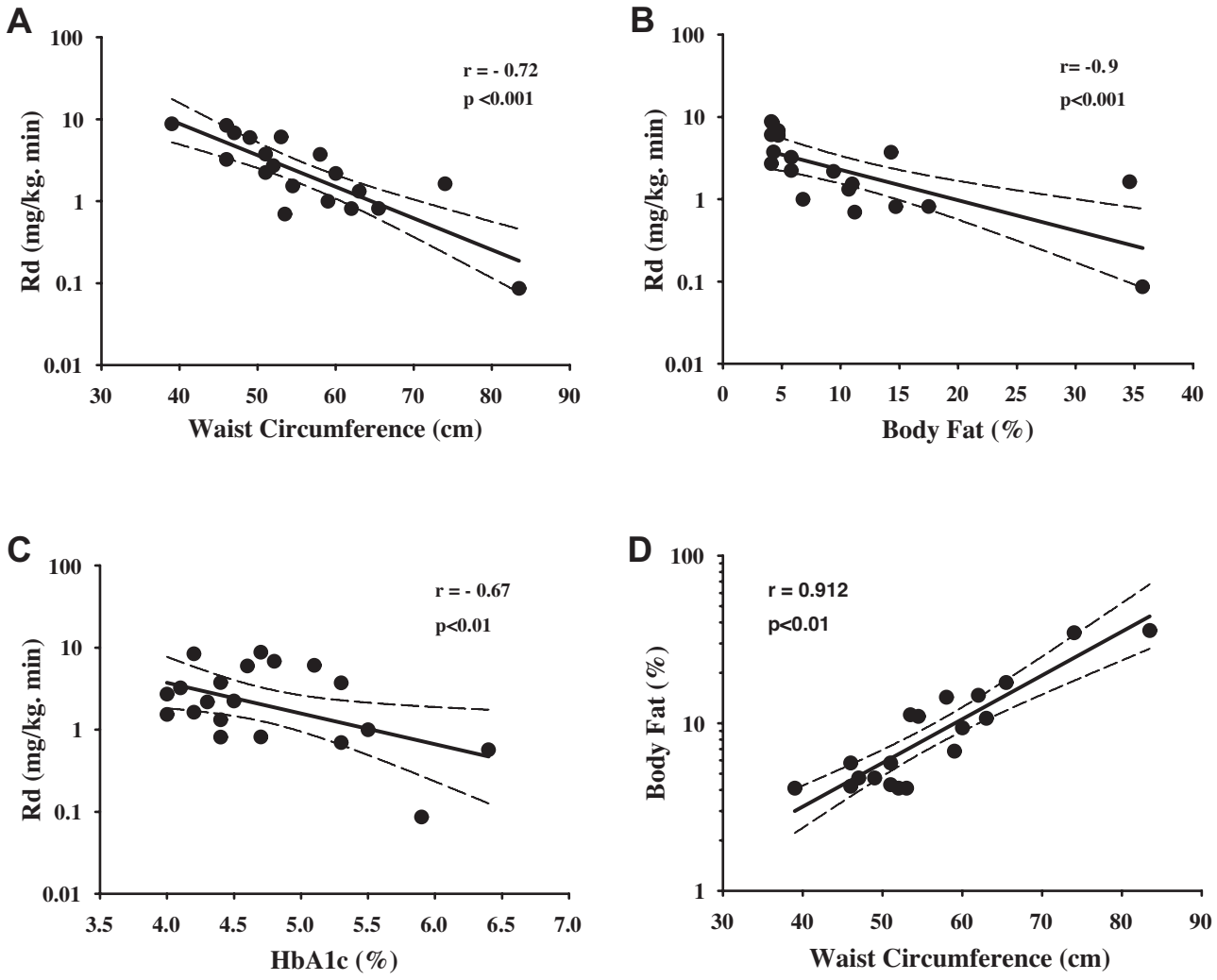

FIG. 2. Partial correlations between R_d versus waist circumference (*A*), percent body fat (*B*), and A1C (*C*) after adjustment for age and sex. The partial correlation coefficient between waist circumference and percent body fat is shown in *D*. The coefficient of determination was adjusted by the number of variables.

basal ($P < 0.05$), whereas there was no increase in IRS-1–associated p85 in the insulin-resistant group. The amount of p85 subunit associated with IRS-1 at 30 min in the insulin-sensitive group was statistically increased compared with the insulin-resistant group ($P < 0.05$; Fig. 3*B*).

Maximal stimulation of Akt phosphorylation in muscle occurred after 120 min of insulin infusion in both insulin-sensitive and insulin-resistant baboons ($P < 0.001$). Akt phosphorylation was significantly reduced in insulin-resistant versus insulin-sensitive baboons at 30 min ($P < 0.05$; Fig. 3*C*). Maximal stimulation of AS160 phosphorylation occurred at 120 min in both insulin-sensitive ($P < 0.001$) and insulin-resistant ($P < 0.05$) groups with a modest, nonsignificant reduction of AS160 phosphorylation in insulin-resistant baboons at 120 min compared with insulin-sensitive baboons (Fig. 3*D*).

In contrast to skeletal muscle, in visceral fat of insulin-sensitive baboons, maximal stimulation of IRS-1 tyrosine phosphorylation occurred at 120 min, and it was significantly different compared with the insulin-resistant group ($P < 0.05$; Fig. 4*A*). There was a nonsignificant trend for an increase in the association of p85 to IRS-1 in the insulin-sensitive baboon group at 120 min (Fig. 4*B*). In the insulin-sensitive baboons, Akt phosphorylation was maximally stimulated at 120 min ($P < 0.001$), and this response was significantly lower in the insulin-resistant group ($P < 0.05$; Fig. 4*C*). In fat from insulin-sensitive baboons, AS160 phosphorylation was maximal at 120 min, and it was significantly lower in the insulin-resistant group ($P < 0.05$; Fig. 4*D*).

TABLE 2
Adjusted correlations between HOMA-β (%) and anthropometric and metabolic markers in the study population

Variable	Correlation coefficient	*P* value
Age (years)	−0.208	0.379
Waist circumference (cm)	0.291	0.227
BMI (kg/m^2)	0.418	0.075
% Body fat	0.519	0.023*
FPG (mg/dl)	−0.03	0.882
A1C (%)	−0.124	0.601
FPI (μU/ml)	0.803	0.001*
Fasting C peptide (ng/ml)	0.600	0.005*
Fasting FFA (μEq/l)	0.616	0.005*
HOMA-IR	0.651	0.002*

*Two-tailed level of significance <0.05.

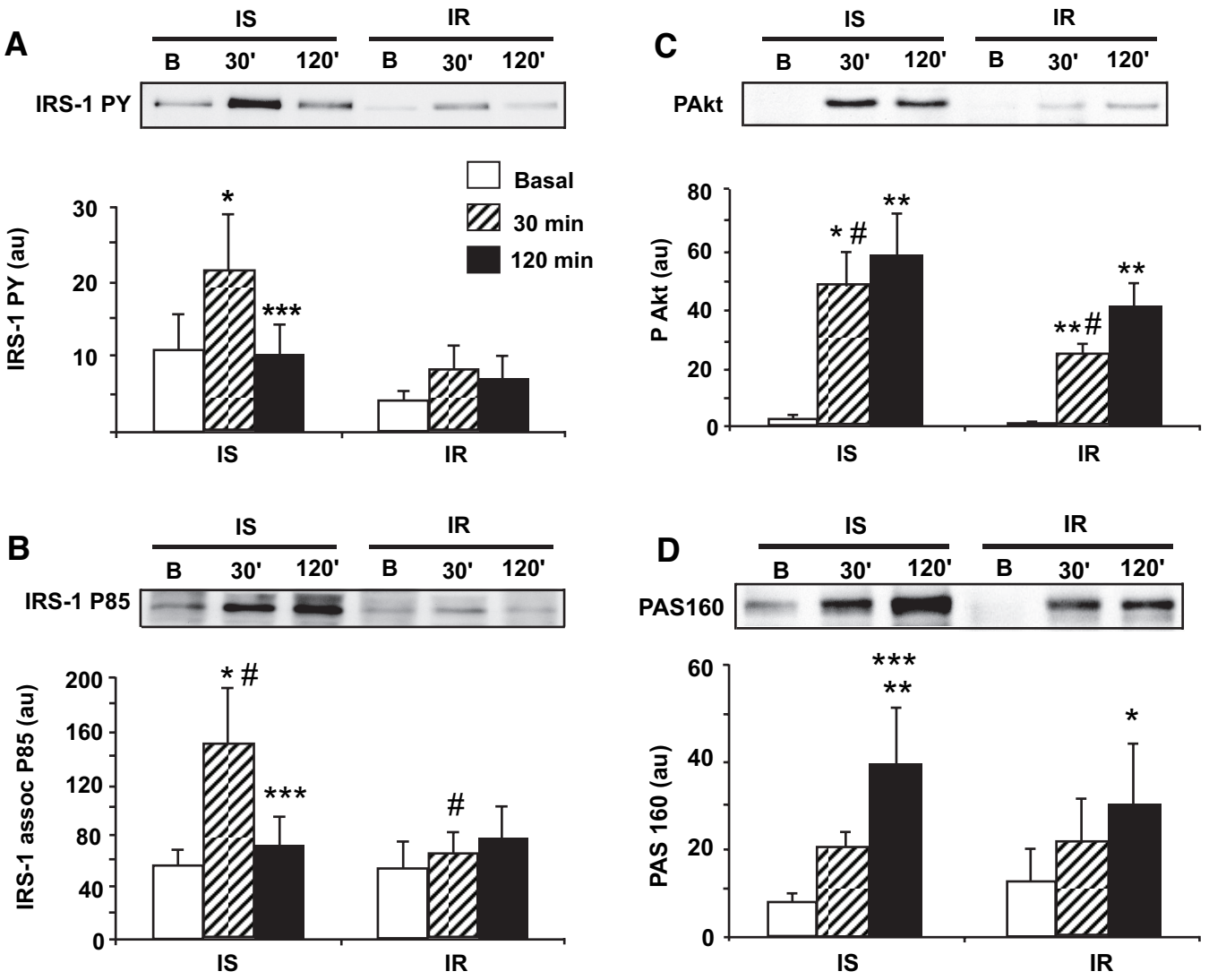

FIG. 3. Insulin signaling in baboon skeletal muscle at baseline and at 30 and 120 min during the euglycemic insulin clamp: IRS-1 tyrosine phosphorylation (PY) (*A*); IRS-1–associated P85 (*B*); Phosphorylation of Akt (Ser473) (P-Akt) (*C*); Phosphorylation of AS160 (P-AS160) (*D*). IS, insulin-sensitive baboons; IR, insulin-resistant baboons. **P* < 0.05 vs. basal level; ***P* < 0.001 vs. basal level; ****P* < 0.05 for 30- vs. 120-min value within a given group; #*P* < 0.05 for 30-min value between groups. *n* = 8 baboons per group.

In the basal state, GLUT1 content in muscle was similar between groups, and there was a nonstatistically significant trend for lower Glut4 muscle content in the insulin-resistant baboons ($P = 0.18$) (Fig. 5*A* and *B*). There were no significant differences in Akt and AS160 muscle content between groups (Fig. 5*C* and *D*). In adipose tissue, there was no change in GLUT4 content between groups. However, we found a nonsignificant decrease in Akt content. Collectively, these results demonstrate that insulin-resistant baboons have major insulin-signaling defects in both muscle and fat.

Gene and protein sequences similarities. The primer sequences are shown as Supplemental Fig. 1*A*–*J* (available in an online appendix at http://dx.doi.org/10.2337/db07-0790). The obtained baboon cDNA sequences had a high degree of identity with the reported human sequences for the analyzed genes. This similarity allows the use of human reagents to study baboon tissues and circulating products (29–31).

We sequenced 73% of the coding region of insulin. This fragment was 95% identical to the human cDNA and 96% to the protein and contains the characteristic insulin-family structure (Supplemental Fig. 2*A*).

We sequenced 100% of the coding region of the insulin receptor. The sequence is 97% identical to the human cDNA and amino acid sequence (Supplemental Fig. 2*B*). The bioinformatics analyses of the sequence identified numerous functional domains, including tyrosine kinase catalytic domains, serine/threonine protein kinase catalytic domains, P-kinase domains, and receptor L domains and furin-like repeats with cysteine-rich regions. The exact function of these domains is not known. Furin is a serine-kinase–dependent proprotein processor.

The coding sequence for baboon IRS-1 was 97% identical to human cDNA and 98% identical at the protein level (Supplemental Fig. 2*C*). Baboon IRS-1 contains a phosphotyrosine binding site and a pleckstrin homology domain, which is characteristic of molecules involved in cell signaling process. Identified functional sites for phosphorylation and other functional sites in the predicted amino acid sequence were found. A deletion of two amino acids was observed in positions 686 and 687 of baboon IRS-1. An

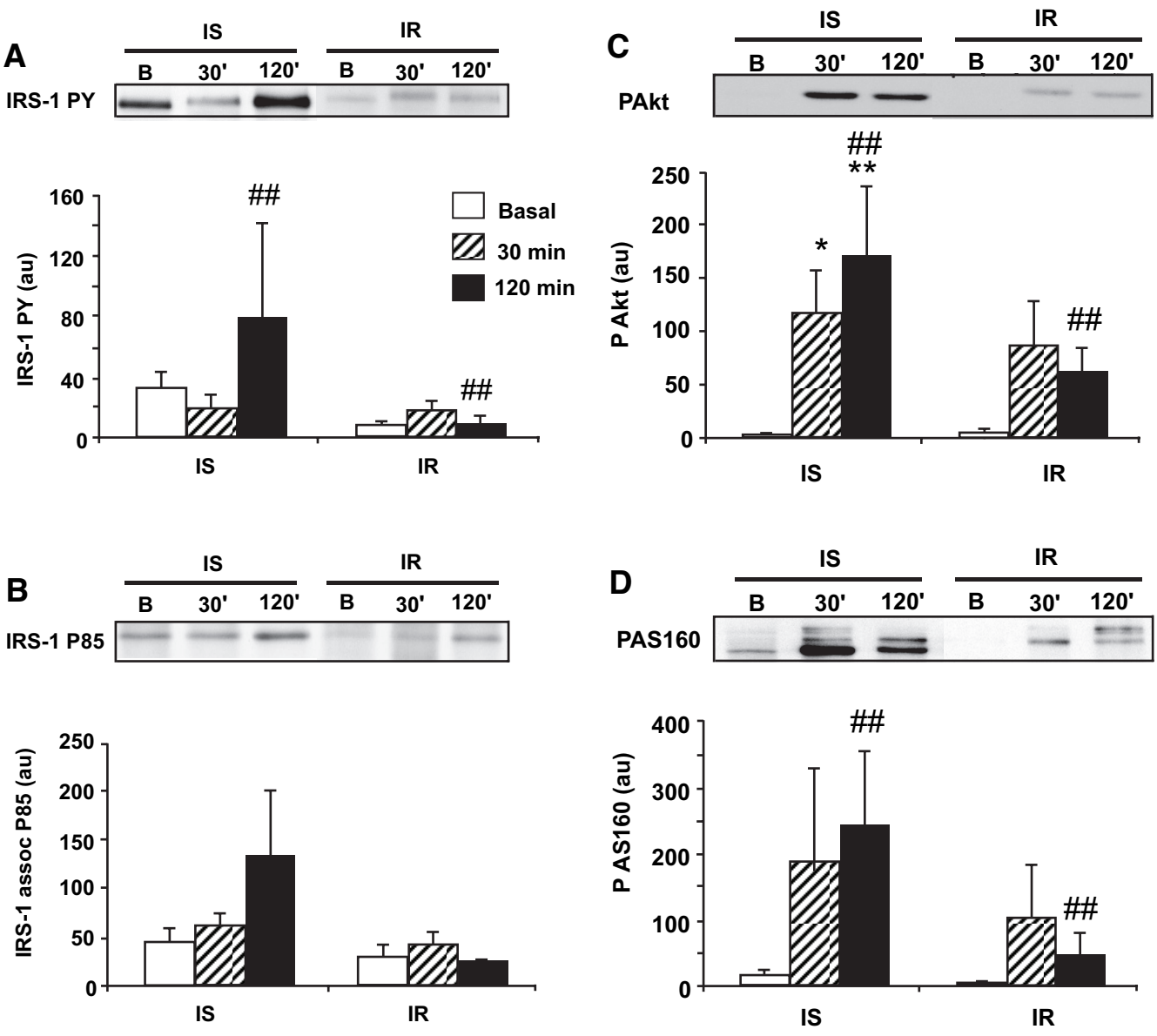

FIG. 4. Insulin signaling in baboon visceral adipose tissue at baseline and at 30 and 120 min during the euglycemic insulin clamp: IRS-1 tyrosine phosphorylation (PY) (*A*); IRS-1–associated P85 (*B*); phosphorylation of Akt (Ser473) (P-Akt) (*C*); phosphorylation of AS160 (P-AS160) (*D*). IS, insulin-sensitive baboons; IR, insulin-resistant baboons. **P* < 0.05 vs. basal level; ***P* < 0.001 vs. basal level; ##*P* < 0.05 for 120-min value between groups. *n* = 8 baboons per group.

insertion of 11 glutamines in positions 881 to 891 and an arginine residue in position 1,231 also were found. No identified functional sites are located within these regions. However, the possible functional effects of these differences remain to be elucidated.

Supplemental Fig. 2*D* shows the alignment of the human baboon protein sequences for phosphatidylinositol 3-kinase (PI 3-kinase). The present sequence covered 95% of the reported human sequence and was 98% identical to the human cDNA and 99% to the protein. The alignments of the baboon and human sequence for p85 are shown in Supplemental Fig. 2*E*. This represents 75% of the human sequence. The percentage of identity between the cDNA is 98 and 99% for amino acid sequences.

In Supplemental Fig. 2*F*, the comparison between the human and baboon AKT-1 is shown. We sequenced 85% of the reported amino acid sequence. This product is 97% identical to the human cDNA and 99% to the human protein. The baboon sequence contains an AKT putative phosphoinositide binding site, a serine/threonine protein kinase catalytic domain and an Akt pleckstrin homology domain. AKT-2 was 99% identical to the human protein (Supplemental Fig. 2*G*). For the AS160 subunit, the sequences were 97 and 98% identical to reported human cDNA and protein, respectively (Supplemental Fig. 2*H*). The baboon sequence for AS160 showed the Pollux phosphotyrosine-binding domain that characterizes this family of molecules across different species. The Trc-2/Bub2/Cdc16 domain was found as well, indicating GTP activator activity. Finally GLUT1 and GLUT4 were 99% identical to the reported amino acid human sequence (Supplemental Fig. 2*I* and *J*). Overall, these baboon genes exhibited highly conserved sequences and functional domains when compared with the reported human proteins.

Transmission electron microscopy. Quantitative analysis showed no differences between insulin-sensitive and

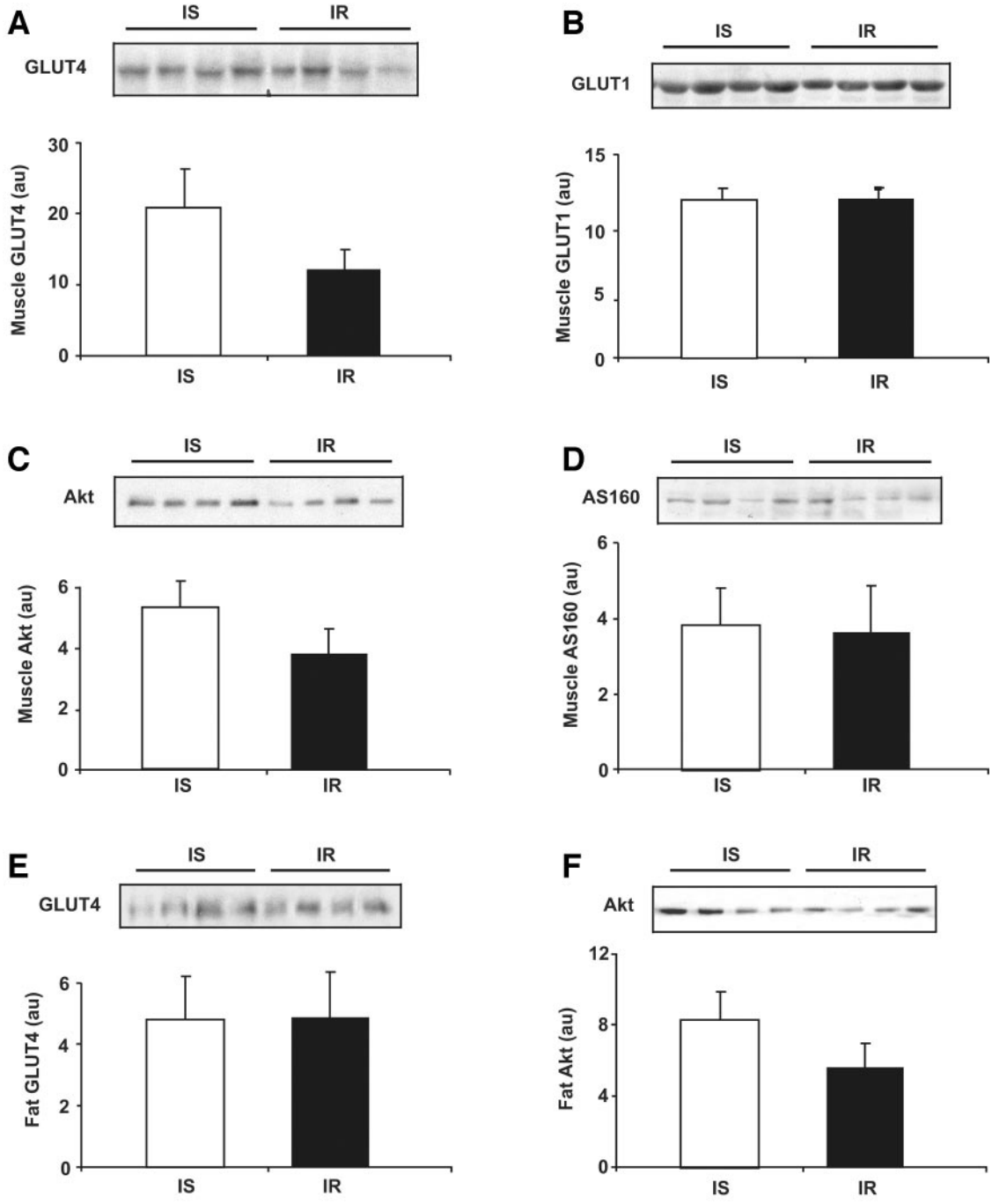

FIG. 5. Basal protein expression differences in target tissues. *A*: GLUT4 expression in skeletal muscle. *B*: GLUT1 in skeletal muscle. *C*: Total Akt in skeletal muscle. *D*: AS160 in skeletal muscle. *E*: GLUT4 expression in adipose tissue. *F*: Akt in adipose tissue. IS, insulin-sensitive baboons (n = 8); IR, insulin-resistant baboons (n = 8).

-resistant baboons in total area occupied by mitochondria (7.5 ± 4 vs. 7.3 ± 3 μm^2, $P = 0.95$), number of mitochondria per field (24 ± 3 vs. 25 ± 10, $P = 0.77$), and average area per mitochondria (0.33 ± 0.19 vs. 0.32 ± 0.10 μm^2, $P = 0.90$). However, qualitative differences were found in morphology, including mitochondrial cristae abnormalities, such as disruption and hyalinization changes in insulin-resistant baboons (Fig. 6*A–D*).

DISCUSSION

In this study, we describe a new nonhuman primate model for the study of insulin resistance. Previous studies have demonstrated that rhesus monkeys become insulin resistant and develop diabetes as they age and become obese (15,19). The present results, as well as those in monkeys, demonstrate that nonhuman primates share many physiological and pathophysiological similarities with humans. We also demonstrate that insulin, insulin receptor, IRS-1, PI 3-kinase, AS160, and AKT are 97–98% similar to human proteins. Although insulin resistance has been demonstrated with the hyperinsulinemic-euglycemic clamp in rhesus monkeys (32,33), the present study represents the first description of insulin resistance and its association with increased adiposity using the insulin clamp technique

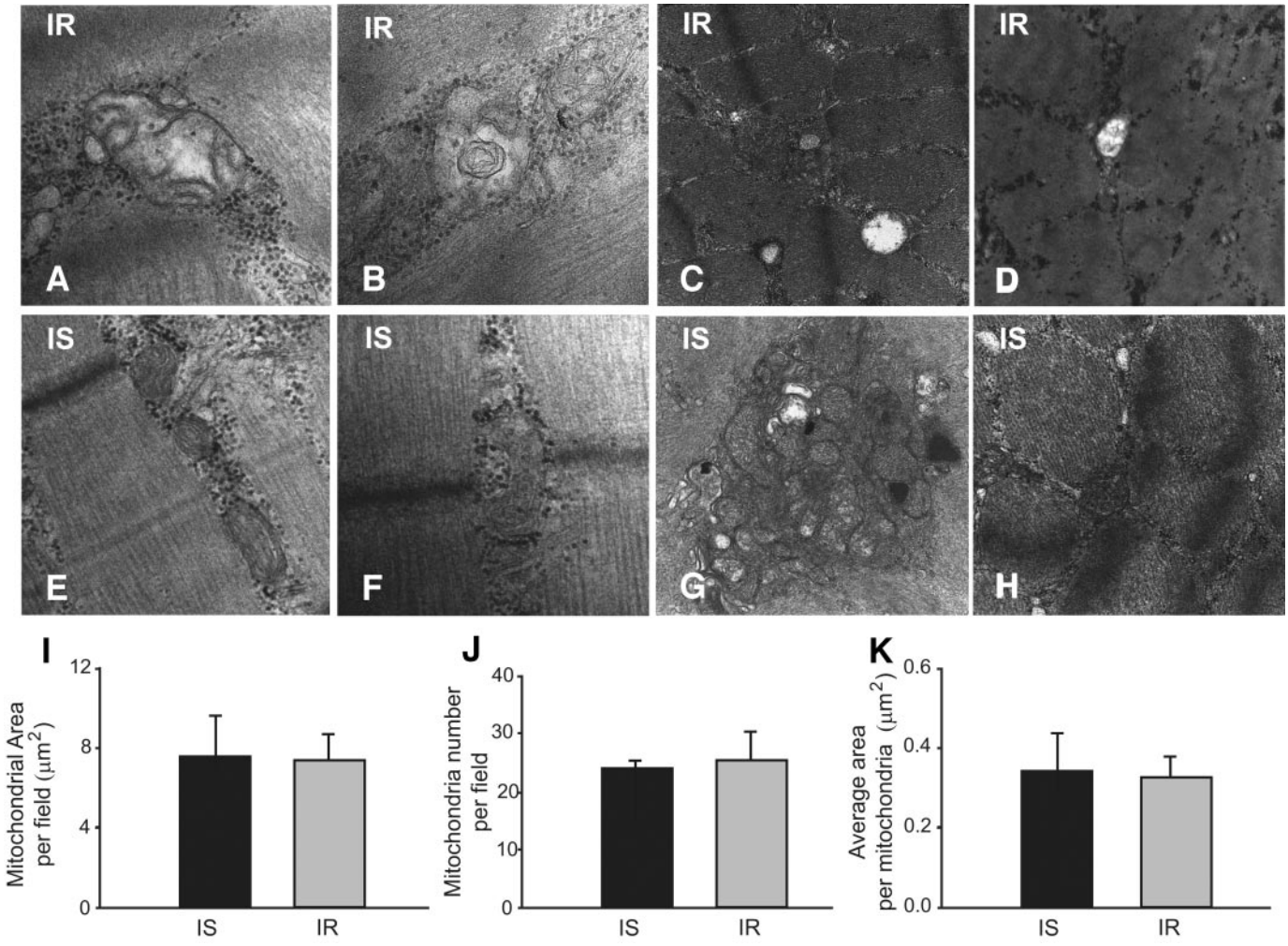

FIG. 6. Mitochondrial morphology in baboon skeletal muscle. Qualitative alterations characterized by cristae disruption and hyalinization changes in the mitochondrial matrix from insulin-resistant animals at magnification ×40,000 (*A*, male; *B*, female) and magnification ×15,000 (*C*, male; *D*, female) compared with the normal mitochondrial morphology from skeletal muscle of insulin-sensitive animals at magnification ×40,000 (*E*, male; *F*, female) and ×15,000 (*G*, male; *H*, female). No differences were found between insulin-resistant and -sensitive baboons in total area covered by mitochondria (*I*), mitochondria number (*J*), and average area per mitochondria (*K*). IS, insulin-sensitive baboons ($n = 8$); IR, insulin-resistant baboons ($n = 8$).

in baboons. Previous work has addressed conditions and markers associated with insulin resistance such as atherosclerosis, dyslipidemia, and obesity in this model (4,12, 27,28). Kemnitz et al. (34) reported that baboons living near tourist facilities in Africa with easy access to calorically dense food had a threefold elevation in fasting plasma insulin, increased body mass, and higher levels of total cholesterol, VLDL, and LDL cholesterol compared with those who consumed only forage and maintained regular physical activity. These observations emphasize the deleterious metabolic effects induced in this primate by changes in lifestyle. Although we did not examine individual patterns of food intake and exercise, it is likely that the change from the wild to captivity explains the development of obesity and insulin resistance in baboons in the present study.

Moreover, we demonstrate that the molecular mechanisms involved in muscle and adipose insulin resistance are similar to those observed in man (35–37) and in other murine models (23,24,38,39). Although Akt and AS160 phosphorylation have been found to be normal in muscle of insulin-resistant nonobese first-degree relatives of subjects with type 2 diabetes (40) in human obesity and type 2 diabetes, the ability of insulin to stimulate IRS-1 tyrosine phosphorylation, increase the association of p85 with IRS-1, and activate P-Akt and P-AS160 are markedly impaired (41–43). Interestingly, we find that insulin-stimulated muscle IRS-1 tyrosine phosphorylation and p85 associated with IRS-1 is maximal at 30 min and dissipates by 120 min. In contrast, we demonstrate that muscle P-Akt and P-AS160 activation continue to increase from 30 to 120 min during the insulin clamp in insulin-sensitive baboons. The effect of insulin on insulin signaling in visceral fat of insulin-sensitive baboons differs markedly from that in muscle (Fig. 4). In insulin-resistant baboons, the ability of insulin to cause IRS-1 tyrosine phosphorylation and to activate PI 3-kinase and distal signaling molecules (P-Akt) is markedly impaired in both muscle and fat tissue. These findings are in general agreement with the above-mentioned studies (41–43), although we cannot exclude the possibility that also other signaling molecules besides Akt might play a role to explain the observed differences between species. As observed in humans, some baboons become obese even though they have been exposed to the same amount and quality of food and have unrestricted physical activity (although probably less than in the wild), provid-

ing support for an inherited metabolic constitution and susceptibility to overweight and development of insulin resistance (4,44). The long lifespan of the baboon and the ability to examine gene-environment interactions makes this animal an interesting model to examine the effect and long-term impact of interventional therapies aimed to treat or prevent insulin resistance, obesity, and type 2 diabetes. Although the primary aim of the present study was to quantitate insulin-mediated glucose disposal and insulin signaling, we estimated HOMA-β as a surrogate marker of β-cell function. Consistent with studies in morbidly obese patients (45), we observed an inverse correlation between HOMA-β and HOMA-IR, BMI, and percent body fat. Of note, and consistent to what has been shown in other primates, the baboon also develops islet amyloidosis and overt diabetes (17,18), similar to that in humans with type 2 diabetes (46,47). Because baboons will not ingest a glucose load, performance of an oral glucose tolerance test is not a feasible option in this primate to estimate insulin secretion.

Although our results demonstrate a significant sexual dimorphism with respect to some plasma lipid levels (FFA, triglyceride, and LDL cholesterol), the insulin-stimulated R_d (marker of insulin resistance) is not affected by sex, and in both males and females, the severity of whole-body insulin resistance is similarly related to the increase in abdominal adiposity. Because waist circumference correlated highly with both % body fat and BMI, the use of anthropometric measurements provides a simple means to identify insulin-resistant baboons. Because the fasting plasma insulin concentration (and consequently HOMA-IR) demonstrates a marked sex dimorphism in our baboon population, these indexes do not represent good surrogate markers of insulin resistance. HOMA-IR is determined by the product of the FPG and FPI concentrations. Because the FPG concentration is primarily determined by the rate of hepatic glucose production and insulin is the major regulator of HGP, HOMA-IR primarily reflects hepatic insulin resistance (48). The 70% lower value for HOMA-IR in females compared with males suggests the presence of significant hepatic resistance that is related to female sex. Because the dose response curve relating the plasma insulin concentration to suppression of HGP is markedly leftward shifted with respect to muscle (49), insulin clamp studies carried out with lower insulin infusion rates and in combination with tritiated glucose are needed to further characterize the hepatic insulin resistance.

In conclusion, the results of the present study support the use of the baboon as a pertinent nonhuman primate model to study the underlying cellular/molecular mechanisms responsible for insulin resistance and to examine pharmacological interventions to reverse it.

ACKNOWLEDGMENTS

This work has received funding from the Kronkosky Charitable Foundation, the National Institutes of Health (grants HL28972 and RR013986), the American Diabetes Foundation, the University of Texas Health Science Center at San Antonio Executive Research Committee, the South Texas Health Research Center, the Nathan Shock Center for Excellence, and the Thai Ministry of Public Health. This investigation was conducted in facilities constructed with support from the Research Facilities Improvement Program (grants C06 RR014578, C06 RR013556, C06 RR015456, and C06 RR017515 from the National Center for Research Resources of the National Institutes of Health).

We thank Michelle M. Leland, DVM, and Stephanie Butler, DVM, for excellent veterinary assistance. We thank Lorrie Albarado and Kimberly Delgado for excellent secretarial assistance.

REFERENCES

1. DeFronzo RA: Pathogenesis of type 2 diabetes mellitus. *Med Clin North Am* 88:787–835, ix, 2004
2. Reaven GM: Why syndrome X? From Harold Himsworth to the insulin resistance syndrome. *Cell Metab* 1:9–14, 2005
3. Muniyappa R, Montagnani M, Koh KK, Quon MJ: Cardiovascular action of insulin. *Endocr Rev* 28:463–491, 2007
4. Comuzzie AG, Cole SA, Martin L, Carey KD, Mahaney MC, Blangero J, VandeBerg JL: The baboon as a nonhuman primate model for the study of the genetics of obesity. *Obes Res* 11:75–80, 2003
5. Rhesus Macaque Genome Sequencing and Analysis Consortium: Evolutionary and biomedical insights from the rhesus macaque genome. *Science* 316:222–234, 2007
6. Wagner JE, Kavanagh K, Ward GM, Auerbach BJ, Harwood HJ Jr, Kaplan JR: Old world nonhuman primate models of type 2 diabetes mellitus. *ILAR J* 47:259–271, 2006
7. Carlsson HE, Schapiro SJ, Farah I, Hau J: Use of primates in research: a global overview. *Am J Primatol* 63:225–237, 2004
8. VandeBerg JL, Williams-Blangero S: Advantages and limitations of nonhuman primates as animal models in genetic research on complex diseases. *J Med Primatol* 26:113–119, 1997
9. Cox LA, Mahaney MC, Vandeberg JL, Rogers J: A second-generation genetic linkage map of the baboon (*Papio hamadryas*) genome. *Genomics* 88:274–281, 2006
10. Rogers J, Hixson JE: Baboons as an animal model for genetic studies of common human disease. *Am J Hum Genet* 61:489–493, 1997
11. Harewood WJ, Gillin A, Hennessy A, Armistead J, Horvath JS, Tiller DJ: Biochemistry and haematology values for the baboon (*Papio hamadryas*): the effects of sex, growth, development and age. *J Med Primatol* 28:19–31, 1999
12. Rainwater DL, Kammerer CM, Cox LA, Rogers J, Carey KD, Dyke B, Mahaney MC, McGill HC Jr, VandeBerg JL: A major gene influences variation in large HDL particles and their response to diet in baboons. *Atherosclerosis* 163:241–248, 2002
13. Cai G, Cole SA, Tejero ME, Proffitt JM, Freeland-Graves JH, Blangero J, Comuzzie AG: Pleiotropic effects of genes for insulin resistance on adiposity in baboons. *Obes Res* 12:1766–1772, 2004
14. Gresl TA, Colman RJ, Havighurst TC, Byerley LO, Allison DB, Schoeller DA, Kemnitz JW: Insulin sensitivity and glucose effectiveness from three minimal models: effects of energy restriction and body fat in adult male rhesus monkeys. *Am J Physiol Regul Integr Comp Physiol* 285:R1340–R1354, 2003
15. Tigno XT, Gerzanich G, Hansen BC: Age-related changes in metabolic parameters of nonhuman primates. *J Gerontol A Biol Sci Med Sci* 59:1081–1088, 2004
16. Stokes WS: Spontaneous diabetes mellitus in a baboon (*Papio cynocephalus anubis*). *Lab Anim Sci* 36:529–533, 1986
17. Hubbard GB, Steele KE, Davis KJ III, Leland MM: Spontaneous pancreatic islet amyloidosis in 40 baboons. *J Med Primatol* 31:84–90, 2002
18. Palotay JL, Howard CF Jr: Insular amyloidosis in spontaneously diabetic nonhuman primates. *Vet Pathol* (Suppl.) 7:181–192, 1982
19. Hansen BC, Bodkin NL: Primary prevention of diabetes mellitus by prevention of obesity in monkeys. *Diabetes* 42:1809–1814, 1993
20. de Koning EJ, Bodkin NL, Hansen BC, Clark A: Diabetes mellitus in *Macaca mulatta* monkeys is characterized by islet amyloidosis and reduction in beta-cell population. *Diabetologia* 36:378–384, 1993
21. DeFronzo RA, Tobin JD, Andres R: Glucose clamp technique: a method for quantifying insulin secretion and resistance. *Am J Physiol* 237:E214–E223, 1979
22. van As A, Lombard F: Body surface area of the Chacma baboon (*Papio ursinus*). *Growth* 45:322–328, 1981
23. Folli F, Saad MJ, Backer JM, Kahn CR: Regulation of phosphatidylinositol 3-kinase activity in liver and muscle of animal models of insulin-resistant and insulin-deficient diabetes mellitus. *J Clin Invest* 92:1787–1794, 1993
24. Folli F, Saad MJ, Backer JM, Kahn CR: Insulin stimulation of phosphatidylinositol 3-kinase activity and association with insulin receptor substrate 1 in liver and muscle of the intact rat. *J Biol Chem* 267:22171–22177, 1992
25. Ritov VB, Menshikova EV, He J, Ferrell RE, Goodpaster BH, Kelley DE:

Deficiency of subsarcolemmal mitochondria in obesity and type 2 diabetes. *Diabetes* 54:8–14, 2005
26. Rizza R, Mandarino LJ, Gerich JE: Dose-response characteristics for effects of insulin on production and utilization of glucose in man. *Am J Physiol* 240:E630–E639, 1981
27. Groop LC, Bonadonna RC, DelPrato S, Ratheiser K, Zyck K, Ferrannini E, DeFronzo RA: Glucose and free fatty acid metabolism in non-insulin-dependent diabetes mellitus: evidence for multiple sites of insulin resistance. *J Clin Invest* 84205–84213, 1989
28. Matthews DR, Hosker JP, Rudenski AS, Naylor BA, Treacher DF, Turner RC: Homeostasis model assessment: insulin resistance and beta-cell function from fasting plasma glucose and insulin concentrations in man. *Diabetologia* 28:412–419, 1985
29. Banks WA, Altmann J, Sapolsky RM, Phillips-Conroy JE, Morley JE: Serum leptin levels as a marker for a syndrome X-like condition in wild baboons. *J Clin Endocrinol Metabol* 88:1234–1240, 2003
30. Tejero ME, Freeland-Graves JH, Proffitt JM, Peebles KW, Cai G, Cole SA, Comuzzie AG: Adiponectin but not resistin is associated with insulin resistance-related phenotypes in baboons. *Obes Res* 12:871–877, 2004
31. Cole SA, Martin LJ, Peebles KW, Leland MM, Rice K, VandeBerg JL, Blangero J, Comuzzie AG: Genetics of leptin expression in baboons. *Int J Obes Relat Metab Disord* 27:778–783, 2003
32. Hotta K, Funahashi T, Bodkin NL, Ortmeyer HK, Arita Y, Hansen BC, Matsuzawa Y: Circulating concentrations of the adipocyte protein adiponectin are decreased in parallel with reduced insulin sensitivity during the progression to type 2 diabetes in rhesus monkeys. *Diabetes* 50:1126–1133, 2001
33. Standaert ML, Ortmeyer HK, Sajan MP, Kanoh Y, Bandyopadhyay G, Hansen BC, Farese RV: Skeletal muscle insulin resistance in obesity-associated type 2 diabetes in monkeys is linked to a defect in insulin activation of protein kinase C-ζ/λ/ι. *Diabetes* 51:2936–2943, 2002
34. Kemnitz JW, Sapolsky RM, Altmann J, Muruthi P, Mott GE, Stefanick ML: Effects of food availability on serum insulin and lipid concentrations in free-ranging baboons. *Am J Primatol* 57:13–19, 2002
35. Morino K, Petersen KF, Shulman GI: Molecular mechanisms of insulin resistance in humans and their potential links with mitochondrial dysfunction. *Diabetes* 55 (Suppl. 2):S9–S15, 2006
36. Cusi K, Maezono K, Osman A, Pendergrass M, Patti ME, Pratipanawatr T, DeFronzo RA, Kahn CR, Mandarino LJ: Insulin resistance differentially affects the PI 3-kinase- and MAP kinase-mediated signaling in human muscle. *J Clin Invest* 105:311–320, 2000
37. Smith U, Axelsen M, Carvalho E, Eliasson B, Jansson PA, Wesslau C: Insulin signaling and action in fat cells: associations with insulin resistance and type 2 diabetes. *Ann N Y Acad Sci* 892:119–126, 1999
38. Mauvais-Jarvis F, Ueki K, Fruman DA, Hirshman MF, Sakamoto K, Goodyear LJ, Iannacone M, Accili D, Cantley LC, Kahn CR: Reduced expression of the murine p85alpha subunit of phosphoinositide 3-kinase improves insulin signaling and ameliorates diabetes. *J Clin Invest* 109:141–149, 2002
39. Kramer HF, Witczak CA, Taylor EB, Fujii N, Hirshman MF, Goodyear LJ: AS160 regulates insulin- and contraction-stimulated glucose uptake in mouse skeletal muscle. *J Biol Chem* 281:31478–31485, 2006
40. Karlsson HK, Ahlsén M, Zierath JR, Wallberg-Henriksson H, Koistinen HA: Insulin signaling and glucose transport in skeletal muscle from first-degree relatives of type 2 diabetic patients. *Diabetes* 55:1283–1288, 2006
41. Pratipanawatr W, Pratipanawatr T, Cusi K, Berria R, Adams JM, Jenkinson CP, Maezono K, DeFronzo RA, Mandarino LJ: Skeletal muscle insulin resistance in normoglycemic subjects with a strong family history of type 2 diabetes is associated with decreased insulin-stimulated insulin receptor substrate-1 tyrosine phosphorylation. *Diabetes* 50:2572–2578, 2001
42. Karlsson HK, Zierath JR, Kane S, Krook A, Lienhard GE, Wallberg-Henriksson H: Insulin-stimulated phosphorylation of the akt substrate AS160 is impaired in skeletal muscle of type 2 diabetic subjects. *Diabetes* 54:1692–1697, 2005
43. Gonzalez E, McGraw TE: Insulin signaling diverges into Akt-dependent and -independent signals to regulate the recruitment/docking and the fusion of GLUT4 vesicles to the plasma membrane. *Mol Biol Cell* 17:4484–4493, 2006
44. Altmann J, Schoeller D, Altmann SA, Muruthi P, Sapolsky RM: Body size and fatness of free-living baboons reflect food availability and activity levels. *Am J Primat* 30:149–161, 1993
45. Dixon JB, Dixon AF, O'Brien PE: Improvements in insulin sensitivity and beta-cell function (HOMA) with weight loss in the severely obese: homeostatic model assessment. *Diabet Med* 20:127–134, 2003
46. Clark A, Wells CA, Buley ID, Cruickshank JK, Vanhegan RI, Matthews DR, Cooper GJ, Holman RR, Turner RC: Islet amyloid, increased A-cells, reduced B-cells and exocrine fibrosis: quantitative changes in the pancreas in type 2 diabetes. *Diabetes Res* 9:151–159, 1988
47. Butler AE, Janson J, Bonner-Weir S, Ritzel R, Rizza RA, Butler PC: β-Cell deficit and increased β-cell apoptosis in humans with type 2 diabetes. *Diabetes* 52:102–110, 2003
48. Tripathy D, Almgren P, Tuomi T, Groop L: Contribution of insulin-stimulated glucose uptake and basal hepatic insulin sensitivity to surrogate measures of insulin sensitivity. *Diabetes Care* 27:2204–2210, 2004
49. Rizza RA, Mandarino LJ, Gerich JE: Dose-response characteristics for effects of insulin on production and utilization of glucose in man. *Am J Physiol* 240:630–639, 1981